AURORA GEOSCIENCES LTD.

MIDNIGHT MINES LTD.

INVERSION OF AEROMAGNETIC DATA IN THE AREA OF THE WOLV & DON PROPERTIES, DONJEK RIVER AREA, YUKON TERRITORY

Mike Power, M.Sc., P.Geoph.

CLAIMS

DON 1-20	YB46996-YB47015
DON 21	YC18523
DON 29-34	YC18531-YC18536
WOLV 1-10	YB46972-YB46981
WOLV 10,12,14, 16, 18	YB46981,3,5,7,9
WOLV 20, 21, 23	YB46991, 2, 4
WOLV 25-28	YC18509-YC18512

Location: 61° 31'N, 139° 49' W
NTS: 115 G/12
Mining District: Whitehorse, YT
Date:02 October 2004

Costs associated with this report have been approved in the amount of $ 3400.00 for assessment credit under Certificate of Work No. QW 27664

Mining Recorder
Whitehorse Mining District

SUMMARY

An automated inversion of total magnetic field data collected over the Wolv and Don Properties was performed to delineate regions of high magnetic susceptibility which might represent ultramafic rock units. An area of 15 km east-west by 11 km north-south covering both properties was selected and digital aeromagnetic data and digital topography covering this area was acquired from the Geological Survey of Canada and the Geodetic Survey of Canada. The data was interpreted using an automated inversion algorithm incorporating an directed conjugate gradient search to generate a three dimensional mesh of elements with varying magnetic susceptibility.

Four runs were performed over a total run time of approximately 36 hours (inversion time only). Three of the models converged to essentially the same general solution and the fourth was rejected because the susceptibilities were out of range. The final model contains a large, apparently folded, magnetic source in the south and a smaller, highly susceptible, depth limited block in the north. This latter feature is interpreted to be a fault bounded block of ultramafic rocks. The model results indicate areas which should be examined more closely with electromagnetic methods.

TABLE OF CONTENTS

LIST OF FIGURES

1.0 INTRODUCTION

Aurora Geosciences Ltd. was retained by Midnight Mines Ltd. to conduct an interpretation of total magnetic field aeromagnetic data collected in the area of the Wolv and Don Properties, Whitehorse Mining District, Yukon Territory. The data was interpreted by employing an automated inversion algorithm to generate a three dimensional (3D) model of the distribution of magnetic susceptibility which may account for the observed magnetic field. This report describes the data set, the inversion procedure, results and an interpretation.

2.0 LOCATION AND ACCESS

The Don and Wolv Properties are centred at 61° 31'N, 139° 49' W, in the southern Yukon Territory (Figure 1). The property is accessible by helicopter from staging points along the Alaska Highway, 15 km to the north of the property. A bulldozer trail in poor condition extends to Arch Creek, 7 km east of the Don Property on the east side of the Donjek River.

3.0 PROPERTY

The Don and Wolv Properties consists of 48 un-surveyed mineral claims staked under the Yukon Quartz Mining Act in the Whitehorse Mining District. Claim information[1] is summarized below:

CLAIM	GRANT NUMBERS	EXPIRY DATE
DON 1-6	YB46996 - YB47001	13 Jan 2008
DON 7-10	YB47002 - YB47005	13 Apr 2006
DON 11-19	YB47006 - YB47014	13 Jan 2008
DON 20	YB47015	13 Apr 2006
DON 21	YC18523	07 Jun 2006
DON 29-34	YC18531-YC18536	07 Mar 2008
WOLV 1,3,5	YB46972, YB46974, YB46976	13 Apr 2006
WOLV 2,4,6	YB46973, YB46975, YB46977	13 Jan 2008
WOLV 7,9	YB46978, YB46980	13 Apr 2006
WOLV 10, 12, 14	YB46981, YB46983, YB46985	13 Jan 2008
WOLV 16	YB46987	13 Jan 2004

[1]Claim information provided by the Whitehorse Mining Recorder on 11 August, 2004.

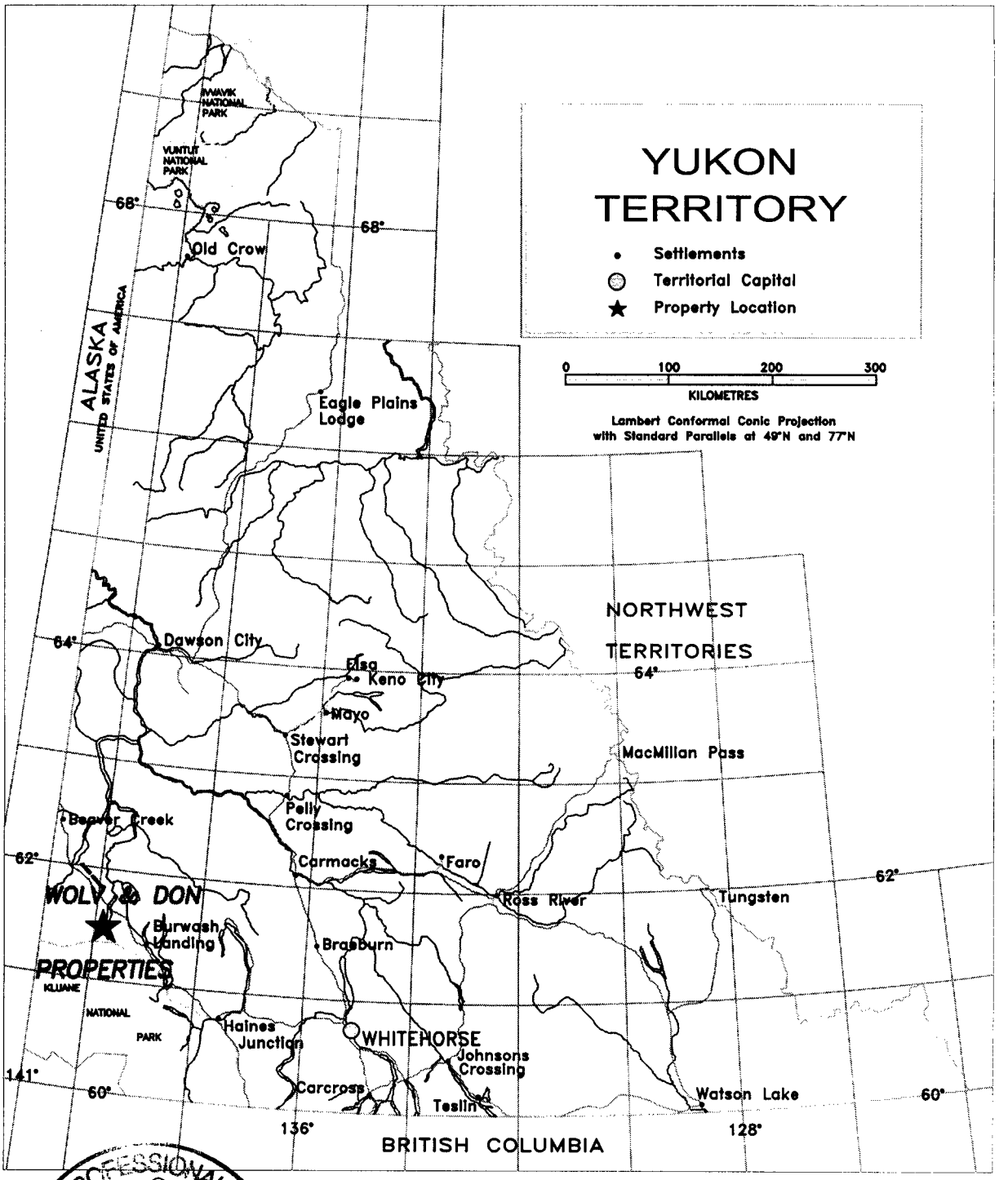

REGISTERED PROFESSIONAL GEOPHYSICIST
M. [illegible]
LICENSEE
N.W.T.

Midnight Mines Ltd.	WOLV & DON PROPERTIES	
PROPERTY LOCATION MAP	MINING DISTRICT: WHITEHORSE	
	SCALE 1: 6,000,000	NTS: N/A
	DATUM: N/A	DRAWN BY: HDS
AURORA GEOSCIENCES LTD.	DATE: 03 October 04	FIGURE: 1

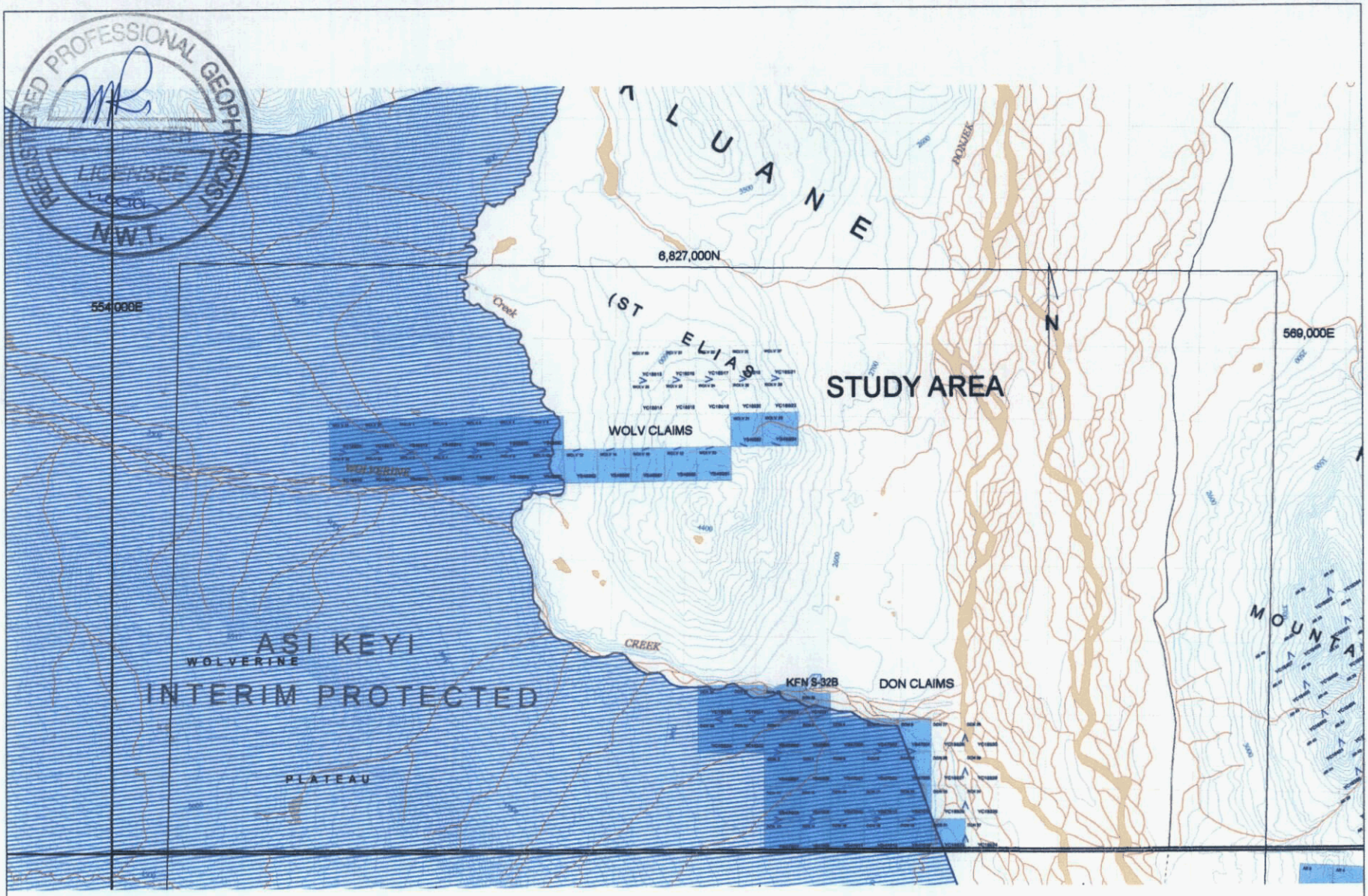

Figure 2. Claim and study area location map.

WOLV 18, 20, 21	YB46989, YB46991-92	13 Apr 2006
WOLV 23	YB46994	13 Apr 2006
WOLV 25, 26	YC18509, YC18510	07 Jun 2006
WOLV 27,28	YC18511, YC18512	07 Mar 2008

Claim locations as shown on government claim maps and the limits of the aeromagnetic data set used in the interpretation are shown in Figure 2.

4.0 PHYSIOLOGY, GEOLOGY AND ECONOMIC MINERALIZATION

The Don and Wolv Properties are situated in Kluane Ranges of the southwest Yukon Territory. Elevations range from 2500 feet in the Donjek River valley to 4500 feet on a hill at the east end of the Wolv Property. The local climate consists of short cool and wet summers from June to early September and cold, dry weather during the winter months of November through April. Vegetation on the property consists of thick willows, spruce and alders.

The regional geology of the property area is summarized by Gordey and Makepeace (1999). The property is underlain by rocks of the Wrangellia Terrane in a fault displaced segment bounded by the Duke River fault south of the property and the Denali Fault System (DFS) to the north.

Rock units mapped in the area of the property are described in Table I. Rock units on the property strike dominantly west-northwest at 300^0 .

Table I. Stratigraphy

Formation (age)	Description
Q Drift (Quaternary)	Glacial overburden; till, moraine, outwash deposits, locally overlain by talus and colluvium.
NW Wrangell Lavas (Miocene - Pliocene)	Phyrric and non-phyrric basaltic andesite flows, interbedded felsic tuff, sandstone and conglomerate.
EKK Kluane Ranges Suite (Late Early Cretaceous	Biotite-hornblende granodiorite, quartz diorite, monzonite.

UTrN Nicolai Formation (Upper Triassic)	Basalt and andesite flows with local tuff, breccia, shale and thin bedded limestone.
CPS1 Skolai Group (Pennsylvanian - Lower Permian)	*Hasen Creek:* argillite, siltstone, greywacke, conglomerate, thin basalt flows. overlies. *Station Creek*: basalt & andesite flows, tuff, agglomerate

In addition, the aeromagnetic signature, limited mapping and prospecting suggests that there may be an intrusion of Kluane Ranges Ultramafic suite rocks on the Don Property. The Kluane Ranges Ultramafic Suite consist of pyroxene gabbro, sheared peridotite, and rare dunite in sills intruding Skolai Group rocks. They may be the hypabyssal precursor to Nicolai volcanic rocks.

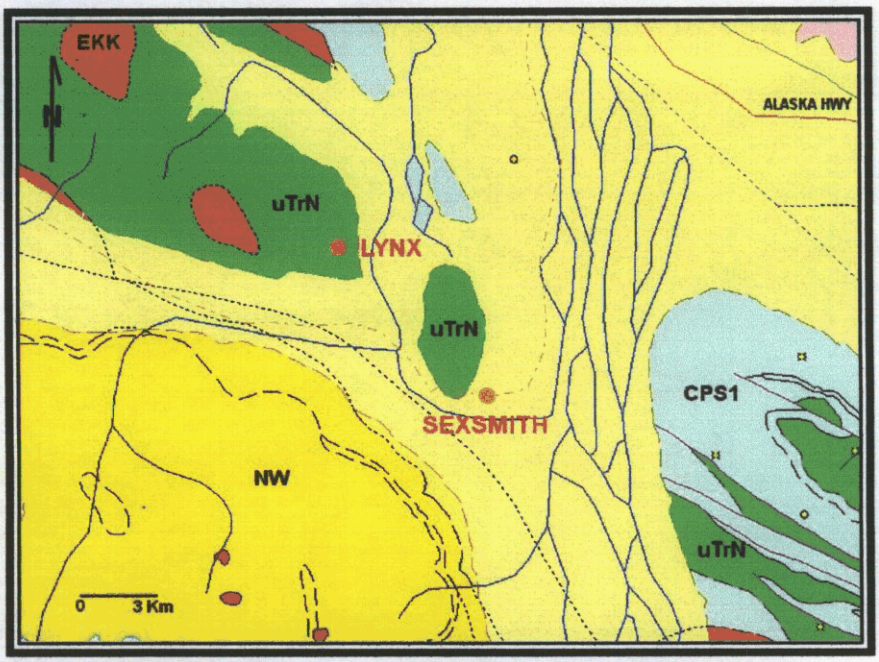

Figure 3. Regional geology (modified after Gordey and Makepiece 1999).

The Wolv Property covers the Lynx Creek (Minfile 115G88) occurrence. The property was staked as the Lynx Claims by AGIP in 1983 but no work was filed. During this period, AGIP and Noranda were exploring gold occurrences in the area of the Wolverine Plateau with attention centred on the Wrangell Lavas.

The Don Property covers the Sexsmith (Minfile 115G33) occurrence. The property was staked by Canalask Nickel Mines Ltd. in June 1953 following an aeromagnetic

survey which located a 1000 nT high. The property was drilled but the work was never filed; old core on the property contains disseminated chalcopyrite in fine grained ultramafic rocks. Both the Don and Wolv Properties were restaked by Expatriate Resources Ltd. in the 1990's. Prospecting on the property in 2001 located samples of magnetite bearing diorite, peridotite, gabbro and andesite flows. (Duncan and Tucker, 2002)

5.0 AEROMAGNETIC DATA

The data set inverted in this study consisted of digitized aeromagnetic data collected for the Geological Survey of Canada from November 1965 to April 1966 by Aero Photo Inc. (GSC 2004).

The surveys were flown according to the following specifications:

Line spacing:	800 m
Flight line azimuth:	0° / 180°
Flight elevation:	305 m above mean terrain elevation
Instrument:	Proton precession (manufacturer not specified)
Platform:	Fixed wing
Sampling:	Not specified; data was manually digitized from analog profiles
Flight path recording:	Film

Figure 4 (back pocket) is a colour contoured total magnetic field map of the study area showing the flight lines and the claim boundaries.

6.0 INVERSION THEORY

The following discussion is based on Telford *et. al.* (1990) and (UBC-GIF (1998). The latter is a description of the inversion algorithm and modelling software.

All magnetic sources are dipolar consisting of positive and negative poles. By convention, a magnetic pole attracted to the north magnetic pole is positive; this is the pole commonly labelled N on compass or other magnets. The south seeking pole is labelled negative. The strength of an external field is measured by placing a unit magnetic pole in the field an observing the force upon it. This vector quantity (magnetic field strength) is commonly labelled **H**. The same magnetic field may also

be produced by a circulating current (Ampere's Law) and consequently **H** is expressed in amperes per metre.

A magnetizable body placed in an external magnetic field will be magnetized by induction. In most cases, the magnetic field induced in a susceptible body (**M**) is uniform and in the same direction as the external field; such a body is uniformly magnetized. The strength of the induced magnetic field in the susceptible object at low magnetic field strengths is linearly related to the external field:

$$\mathbf{M} = k\mathbf{H}$$

where k is the magnetic susceptibility of the object. Susceptibility is measured in dimensionless SI units. In the earth, k varies from about 0.0001 in non-susceptible rocks to 0.5 in highly susceptible rocks. The table below, adapted from Telford *et. al.* (1990) shows the common range of relative magnetic susceptibilities exhibited by various common rocks and minerals. Note that the susceptibilities are expressed in SI units x10^3 to make the ranges more apparent.

Table II. Average magnetic susceptibility of common rocks and magnetic minerals after Telford *et. al.* (1990)

Rock / mineral	**Range (SI units x10^3)**	**Average (SI units x10^3)**
Carbonates	0 - 3	0.3
Sandstone	0 - 20	4.0
Shale	0.01-15	0.6
Granite / rhyolite	0 - 80	8
Diorite	0.6 - 120	85
Andesite	not reported	160
Basalt	0.2 - 175	70
Gabbro	1 - 90	70
Peridotite	90- 200	150
Magnetite	1200 - 19200	6000
Pyrrhotite	1 - 6000	1500
Ilmenite	300 - 3500	1800
Chromite	3 - 110	7
Hematite	0.5 - 35	6.5

Average non-ferrous	0 - 3	0.2

The magnetic induction (**B**) is the total field created by both the external field and the induced field. This slightly misleading denomination is used because the external field is also considered to create an induced field in free space which has a susceptibility $\mu_0 = 4\pi \times 10^{-7}$ and thus the total field is:

$$B = \mu_0(\mathbf{H}+\mathbf{M}) = \mu_0(1+k)\mathbf{H}$$

It is readily apparent that the external (earth's) field is amplified in the presence of a body with magnetic susceptibility.

In broad terms, the earth's external field consists of a dipole with north and south poles and with large scale secondary features in the order of thousands of kilometres due to deep-seated magnetic features in the mantle and core. The earth's field is a vector quantity having both magnitude (the total field strength) and direction (inclination and declination - the angles with respect to vertical and to geodetic north). The earth's field is mathematically approximated by the International Geomagnetic Reference Field (IGRF) - a formulation of the earth's magnetic field in spherical coordinates using Legendre Polynomials to approximate the external field due to large scale features in the earth's mantle and core. If the effect of the earth's field is removed from a data set by calculation and subtraction, the remnant field due to shallow sources is termed the residual field.

For the purposes of this discussion, the anomalous magnetic field to be inverted is the residual field and the magnetic effects in the model are caused solely by magnetic induction. The induced magnetic field is presumed to be parallel to the external field and there is no remnant magnetization. In this study, the inversion software models the total field strength only.

The inversion software calculates the total magnetic field anomaly at any point by dividing the model into a 3D distribution of rectangular cells. The total magnetic field contribution of each cell is calculated using the numerical expressions for the magnetization of a rectangular prism developed by Bhattacharyya (1964). Consider the case of an external field H_p with direction cosines l, m, and n, and a rectangular prism centred at point (x_0, y_0, z_0 (=h)), with prism lower and upper bounding points (x_l, y_l, z_l) and (x_u, y_u, z_u) and internal polarization vector direction cosines L, M, and N. The anomalous field at observation point (x,y,z) for the single rectangular prism element can be evaluated numerically using:

$$T = H_p \left[\begin{array}{l} \dfrac{a_{23}}{2}\log\left(\dfrac{r_0 - a_1}{r_0 + a_1}\right) + \dfrac{a_{13}}{2}\log\left(\dfrac{r_0 - b_1}{r_0 + b_1}\right) - a_{12}\log(r_0 - h_1) \\ -lL\tan^{-1}\left(\dfrac{a_1 b_1}{a_1^2 + r_o h + h^2}\right) - mM\tan^{-1}\left(\dfrac{a_1 b_1}{r_0^2 + r_0 h - a_1^2}\right) \\ +Nn\tan^{-1}\left(\dfrac{a_1 b_1}{r_0 h}\right) \end{array} \right] \Bigg|_{x_l}^{x_u} \Bigg|_{y_l}^{y_u}$$

where

$$a_{12} = Lm + Ml$$
$$a_{13} = Ln + Nl$$
$$a_{23} = Mn + Nm$$
$$r_0^2 = (x - x_0)^2 + (y - y_0)^2 + h^2$$
$$a_1 = x - x_0$$
$$b_1 = y - y_0$$

The calculations are simplified slightly by the fact that the polarization vector in each element is assumed to be parallel to the external earth's field (ie. there is no demagnetization effect and no remnant magnetization). Consequently,

$$l = L$$
$$m = M$$
$$n = N$$

The observed field at any point above the 3D susceptibility model is the vector sum of the magnetization from each prismatic volume element in the model. The model mesh normally consists of large, widely spaced cells in the areas surrounding the region where the data is located and at depth below the likely range of investigation of the data. These padding cells are necessary to prevent sharp edge effects where the susceptibility would otherwise be zero. Normally, these cells are removed in displaying the final model to concentrate the reader's attention on that area of the model where the data is strongly controlling the susceptibility distribution. In addition, the inversion process can incorporate topography into the final model by setting all cells which are above the ground surface to a null-value (ie. not to be used in the calculation).

To determine an optimum solution, it is first necessary to determine the how

changes in the model create changes in the observed field at the stations at surface. This can be done by defining a sensitivity matrix **G** relating the measurements **d** and the susceptibility of the model elements **k**:

$$\mathbf{d} = \mathbf{Gk}$$

The sensitivity matrix can be very large with dimensions equal to the product of the number of cells in the 3D model and the number of measurements. To minimize the computational and storage burden, the program compresses this sparse matrix by only recording the elements which have discernible effects on the data.

The inversion algorithm attempts to create a 3D model of susceptibility which has a response which agrees with the field data within the bounds of measurement error, and which incorporates a minimum degree of complexity. An inherent assumption in the inversion process is the assumption that, in general, the model with the least complexity is the best solution to the inversion problem. It is possible to over-model data by generating fine details in the model which have little or no effect on the model response. The model should also incorporate any assumptions about the decay of the magnetic field with depth and information on any preferred orientation for magnetic features. To guide the generation of a geophysically meaningful model, we define a model objective function which, when minimized, indicates that the inversion process has generated a valid model.

The model objective function is minimized when it has generated a model which is "close" to a reference model $\mathbf{m_0}$ and which is smooth in all three (x,y,z) directions. The objective function also incorporates weighting functions for the three directions (w) and coefficients expressing the relative importance of different components in the objective function (α). The general form for this model objective function is:

$$\phi_m(m) = \alpha_s \int_V w_s \left\{ w(\mathbf{r})\left[m(\mathbf{r}) - m_o\right]\right\}^2 dv + \alpha_x \int_V w_x \left\{ \frac{\partial w(\mathbf{r})\left[m(\mathbf{r}) - m_o\right]}{\partial x} \right\}^2 dv$$

$$+ \alpha_y \int_V w_y \left\{ \frac{\partial w(\mathbf{r})\left[m(\mathbf{r}) - m_o\right]}{\partial y} \right\}^2 dv + \alpha_z \int_V w_z \left\{ \frac{\partial w(\mathbf{r})\left[m(\mathbf{r}) - m_o\right]}{\partial z} \right\}^2 dv$$

where the functions w_s, w_x, w_y and w_z are position dependent weighting functions and α_s, α_x, α_y and α_z are coefficients which bias the relative importance of different elements in the weighting function. w(r) is a generalized depth weighting function implemented to counteract the geometrical decay of sensitivity with distance from the observation point. This function prevents the recovered susceptibility from being concentrated near the observation point. m_o is a reference model with which the developing model is compared in order to loosely constrain a final solution to some general region of the solution space - at least in those portions of the model not

strongly controlled by sensitivity to the data. By changing the relative weights of the α coefficients, the developing model can be forced to generate features which are elongated in the direction of the coefficient with the largest weighting. For example, if vertical features are known to be present, α_z could be weighted at 5 while the other coefficients could be left at 1 to force the model to preferentially generate vertical features. The coefficient α_s is a measure of the degree to which the model is forced to approximate the reference model; if α_s is small, the model norm is not especially sensitive to deviations from the reference model. In practice, the reference model is a constant average of the estimated half space magnetic susceptibilities. Consequently, using default reference models, a large value of α_s causes a minimized model norm to approximate a simple half space. Under-weighting α_s allows the model to generate compact small scale features to replicate the observed field. In other situations where a reference model generated from a geological cross section or some other *apriori* data is used, varying α_s will govern the extent to which the inversion model will be allowed to drift from this preferred region of the solution space.

To numerically implement the model norm, this function is discretized using a finite difference mesh defining the susceptibility model:

$$\phi_m = (m - m_0)^T \left(W_s^T W_s + W_x^T W_x + W_y^T W_y + W_z^T W_z\right)(m - m_0)$$
$$\equiv (m - m_0)^T \left(W_m^T W_m\right)(m - m_0) = \left\| W_m (m - m_0) \right\|^2$$

in which the individual weighting matrics W_s, W_x, W_y, and W_z are calculated from the weighting functions once the model mesh has been defined. To assess the misfit between the magnetic field generated by the model and the observed magnetic field, the 2D norm is used as a misfit:

$$\phi_d = \left\| W_d \left(G_k - d^{obs}\right) \right\|^2$$

in which W_d is the weighting matrix of the observations. If the noise in the data is assumed to Gaussian, we use the inverse of the standard deviation in magnetic field repeat measurements in the weighting matrix. If the weighting matrix perfectly compensates for the error in the data, the target misfit for the data set is N where N is the number of data points.

The depth weighting function is incorporated into the weighting matrix $\mathbf{W_m}$. Magnetic field data collected at surface is inherently insensitive to depth; a given magnetic field anomaly could be produced by a wide range of sources - some compact with high (or low) magnetic susceptibility near surface or, alternatively, extended deep sources with lower magnetic susceptibility. The inherent non-uniqueness of depth solutions to magnetic field problems requires that the inverter specify some method of dealing with this source of uncertainty. Intuitively, this requires a weighting of

deeper cells to the cancel the decay in deep cell influence on the final solution and thereby allow the deeper cells to enter into the solution with a nonzero susceptibility. In the case of data collected at the earth's surface, a $1/z^3$ decay is observed and the weighting function can be framed as:

$$w(\mathbf{r}_j) = \left[\frac{1}{\Delta z_j} \int_{\Delta z_j} \frac{dz}{(z + z_o)^{\beta}} \right]^{0.5} \quad (j = 1,2,3 \ldots M)$$

where M is the number of cells in the mesh. β is commonly set to 3.0 in most inversions but can be varied by the interpreter in situations where a pseudo-monopole field might be expected (eg. some distance above a very large source in a vertical magnetic field).

The optimum solution to the geophysical problem is to generate a geophysically plausible model (minimize model objective function) and to explain the observed data by replicating it (achieve desired misfit). Formally, the inverse problem can be framed as minimize:

$$\phi = \phi_{\mathrm{d}} + \xi \phi_{\mathrm{m}} - 2\lambda \sum_{j=1}^{M} \ln(m_j)$$

subject to:

$$m > 0$$

where ξ is a tradeoff parameter which the controls the relative importance of the model norm and the data misfit and **m** is the matrix of model elements. The final term in the expression for ϕ is a logarithmic barrier expressing the positivity constraint. By definition, magnetic susceptibility is a positive number and negative solutions are not physically plausible. Implementing this constraint in the solution search by a sharp logic term (ie. if negative, reject) would provide no input to the objective function as to where to search for a solution. Instead a logarithmic barrier is erected to prevent the model from generating negative solutions.

The inversion program implements the conjugate gradient algorithm with forced positivity to search for an optimum solution. The program iteratively adjusts the susceptibility of each element to minimize ϕ by noting the gradient in ϕ as a function of each element in the sensitivity matrix. The coefficient λ in the logarithmic barrier is gradually reduced as the program converges on a solution in a region of solution space where all model elements are positive.

The determination of a trade-off parameter is important. In general, the trade-off parameter will be high for noisy data and small for data with little measurement error. The standard deviation of the total magnetic field measurements is not

known and can only be roughly estimated from the instrument specifications because the atmospheric noise, correction errors, and the effect of geographic location error are not known. If this error were known, the sum of the squared error would be used to determine a trade-off parameter which minimized f. In the absence of reliable measurement error information, x must be determined using one of three strategies:

1. Chi-factor

2. Constant trade-off

3. Generalized cross validation (GCV)

Option 1 assumes that the errors are well known and thus x can estimated directly from the number of measurements. Option 2 searches a three dimensional solution space occupied by f_d, x and f_m to find a minimum value of all three. This strategy is computationally intense and the process is expedited by relaxing the positivity constraint to capitalize on the fact that x curves near a solution follow the same curve regardless of whether positivity is constrained or not. Relaxing the positivity constraint greatly speeds up the computations and this is done to determine the slope of solution space near the correct ξ in a first pass. In a second pass with positivity, this information is used to quickly converge to a valid solution which minimizes all three variables in the inversion. Option 3 (GCV) is a statistical technique used to estimate the error in the absence of reliable error determinations. In this implementation, it is applied without positivity and the estimate of ξ is then used in a final solution with positivity. It is useful if the data does not have a strong negative bias and are not sparsely distributed.

7.0 INVERSION PROCEDURES

The data was processed with Geosoft™ Ver. 5.01 and inverted with the UBC -GIF Mag3D program described in the previous section. The following data processing and inversion procedures were used to generate the final models:

1. Digital aeromagnetic data was transformed to NAD 83 UTM Zone 7N coordinates.

2. The aeromagnetic data was gridded using a 200 m cell size to generate a uniform representation of the geomagnetic field over the study area. A default error of 0.1 nT was assigned to each reading. This aeromagnetic data was exported as an ASCII data file (observations file).

3. A digital elevation model was constructed covering the study area. Digital topographic maps were acquired in AutoCadd Rel. 14 format and were transformed to Rel 12 DXF format. Contour information was extracted from

the DXF file in the form of individual contour endpoints. The locations of these points are in UTM coordinates (NAD83) and the elevation of these points are geodetic elevations above mean sea level in feet. The elevations were transformed to elevations in metres ASL and the data set was entered as point data into Geosoft where it was gridded using a 200 m cell size. The grid was exported as an ASCII digital elevation model of the study area (topography file).

4. The earth's geomagnetic field at the date of the survey was modelled using the IGRF and the field parameters (strength, inclination and declination) merged with the magnetic field data in the observations file.

5. A model mesh was specified. This consisted of an 81 (EW) x 51 (NS) x 58(z) mesh of 239,598 cells (including padding cells) covering an area of 17.8 km (EW) x 11.8 km (NS) x 14.8 km (deep). The smallest cells were in the centre of the model and these were 200 m x 200 m x 100 m (thick).

6. A series of 4 inversions were run using the parameters listed below:

Run 1

Trade-off parameter method:	chi factor 1.0
α_s α_x α_y α_z :	0.0001, 1,1,1
Depth or distance weighting:	Depth
Depth weighting coefficient:	3.0
Wavelet compression:	Default
Initial model:	Default
Reference model:	Default

Run 2

Trade-off parameter method:	GCV
α_s α_x α_y α_z :	0.0001, 1,1,1
Depth or distance weighting:	Depth
Depth weighting coefficient:	3.0
Wavelet compression:	Default
Initial model:	Default

Reference model:	Default

Run 3

Trade-off parameter method:	GCV
α_s α_x α_y α_z :	0.0001, 1,1,5
Depth or distance weighting:	Depth
Depth weighting coefficient:	3.0
Wavelet compression:	Default
Initial model:	Default
Reference model:	Default

Run 4

Trade-off parameter method:	Constant - 1.0
α_s α_x α_y α_z :	0.0001, 1,1,5
Depth or distance weighting:	Depth
Depth weighting coefficient:	3.0
Wavelet compression:	Default
Initial model:	Default
Reference model:	Default

The inversions required approximately 36 hours of inversion time on an Athlone 2.6 Ghz computer running Windows XP.

8.0 RESULTS

The range of model magnetic susceptiblities is a preliminary gauge of the results of the inversions. These are tabulated below:

Run	Susceptibility range (SIx10^{-3})
1	0 - 675
2	0 - 587
3	0 - 448
4	1700 - 12800

It is readily apparent that the final run produced a model with unrealistic magnetic susceptibilities. The remaining models are generally similar in their broad features.

Run 3 was selected as the best run although this run was very similar to Run 2. Run 1 generated more localized outliers than either Runs 2 or 3; consequently it was rejected. The following discussion describes the features of the model generated in Run 3.

The primary target of mineral exploration on the Don and Wolv Properties is ultramafic hosted Ni-Cu-PGE massive sulphide bodies. Consequently, model display parameters are adjusted to preferentially indicate the location of magnetic sources with properties within the range expected for ultramafic rocks. The colour bar is scaled from 0.070 to 0.150 SI units to show susceptibilities in the basalt / gabbro range as blue, and those in the peridotite - pyroxenite range as red. The model cutoff has been set at 0.070 SI units and only those cells which have susceptibilities above this value are shown. This cutoff is the average magnetic susceptibility of gabbroic rocks; peridotite, dunite and pyroxenite usually have higher magnetic susceptibilities. Thus, to a first approximation, those regions which are hot coloured (red end of the spectrum) have susceptibilities in the pyroxenite - peridotite range while those which are blue are in the basalt - gabbro range. UTM coordinates are displayed along the model horizontal axis while the vertical axis is elevation above mean sea level in metres. Horizontal padding cells have been removed so that the model covers only the area covered by the data (ie. the study area).

Figure 5 is a comparison between the observed data (GSC data) and the model response (the total magnetic field generated by the model). It is readily apparent that the final model replicates all the essential features of the GSC data.

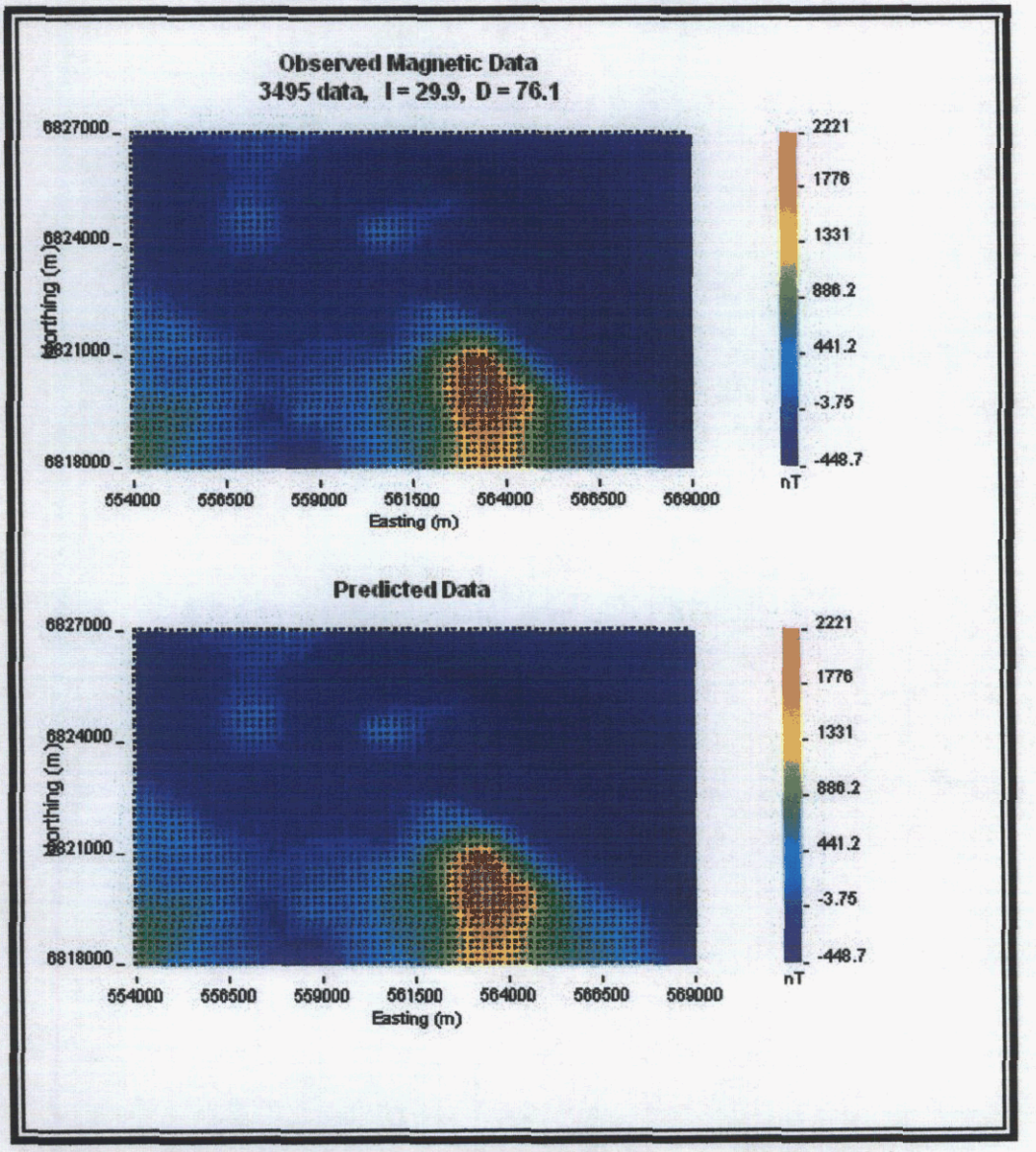

Figure 5. Observed data and data predicted by the final model.

Figure 6 is a top view of the model. There is a prominent magnetic source in the southern portion of the model which is coincident with the Don Property. In addition, there is a small northern outlier of magnetic material. Figures 7 through 10 are views of the model from the south, west, north and east sides respectively.

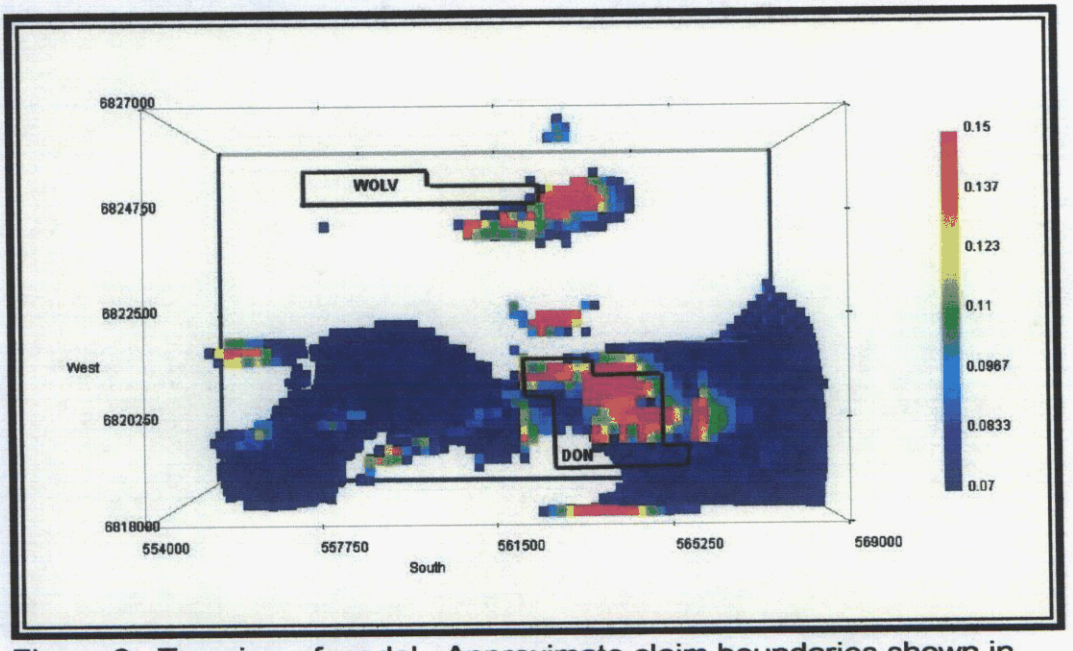

Figure 6. Top view of model. Approximate claim boundaries shown in black.

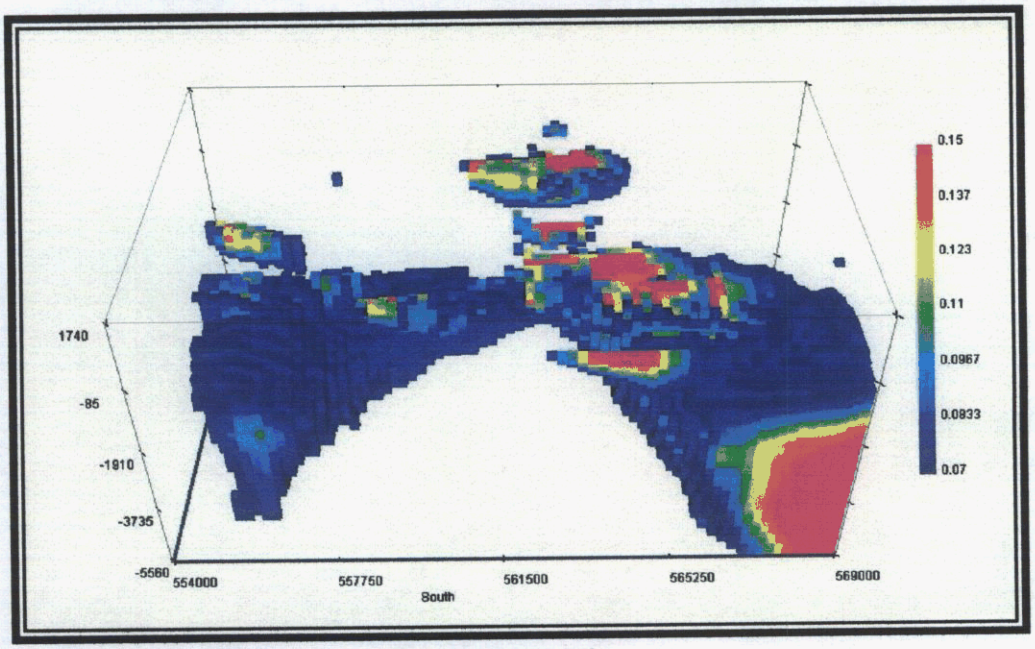

Figure 7. Model viewed from upper south.

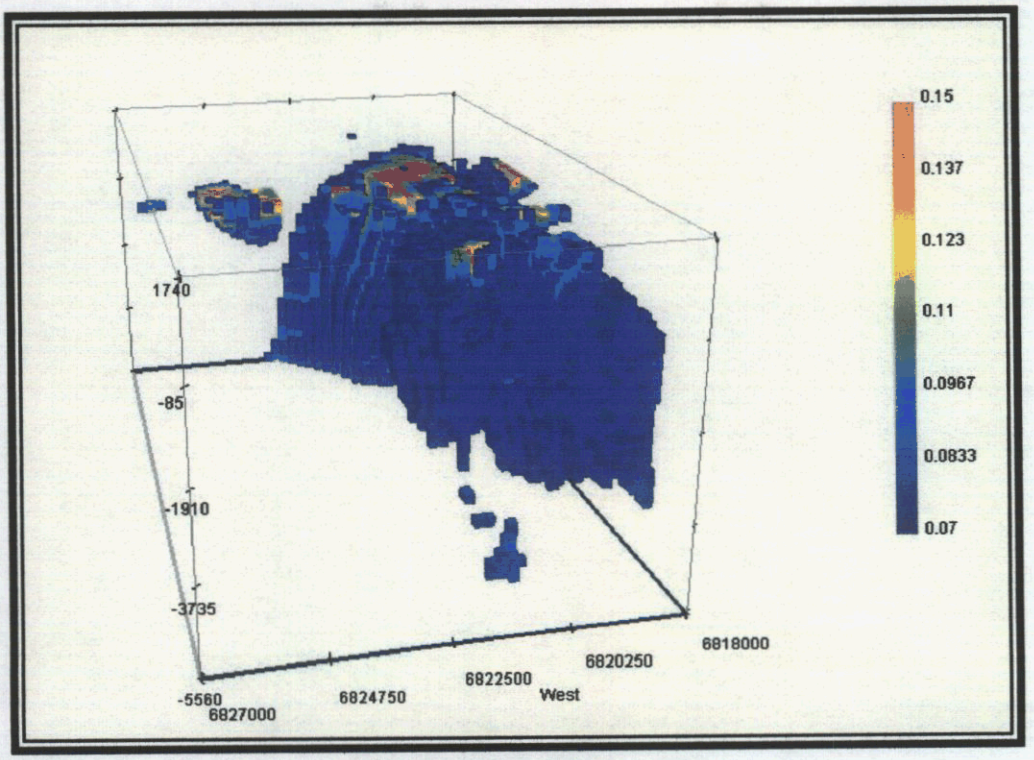

Figure 8. Model viewed from west, above

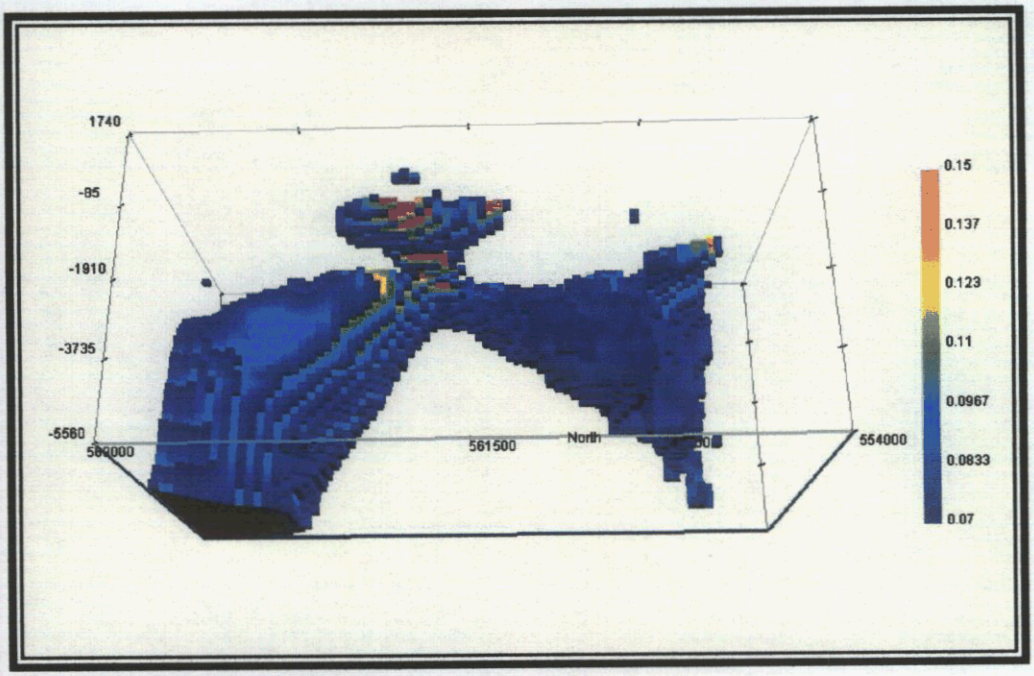

Figure 9. Model viewed from north, below

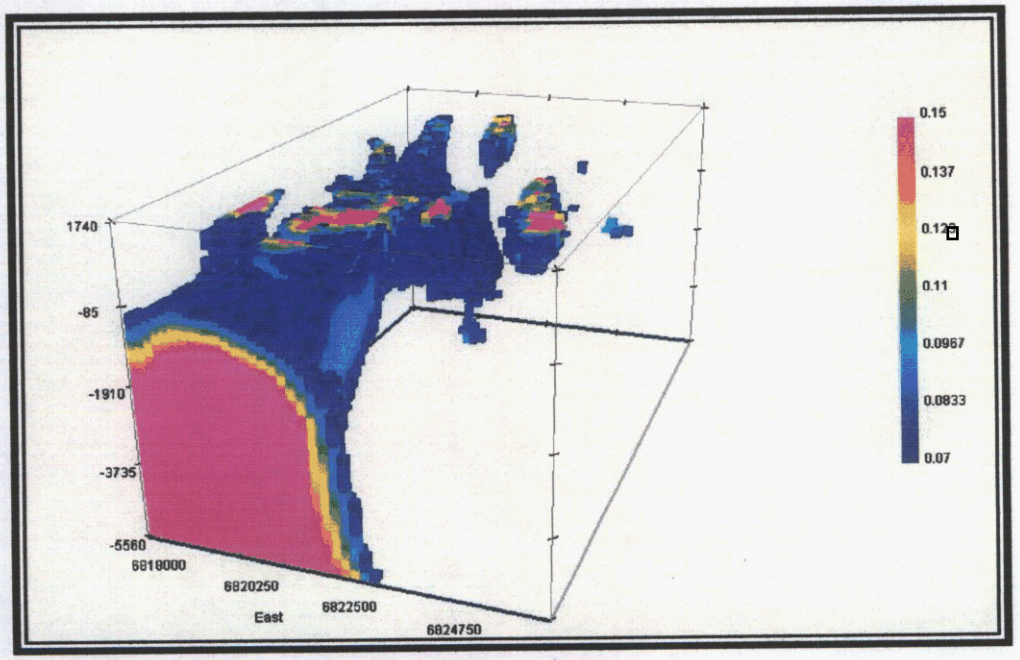

Figure 10. Model viewed from east, above

Figure 11 is a detail cut along easting 563,800E showing, in cross section from south (left) to north (right), the depth extent of the main southern magnetic source and the northern outlier.

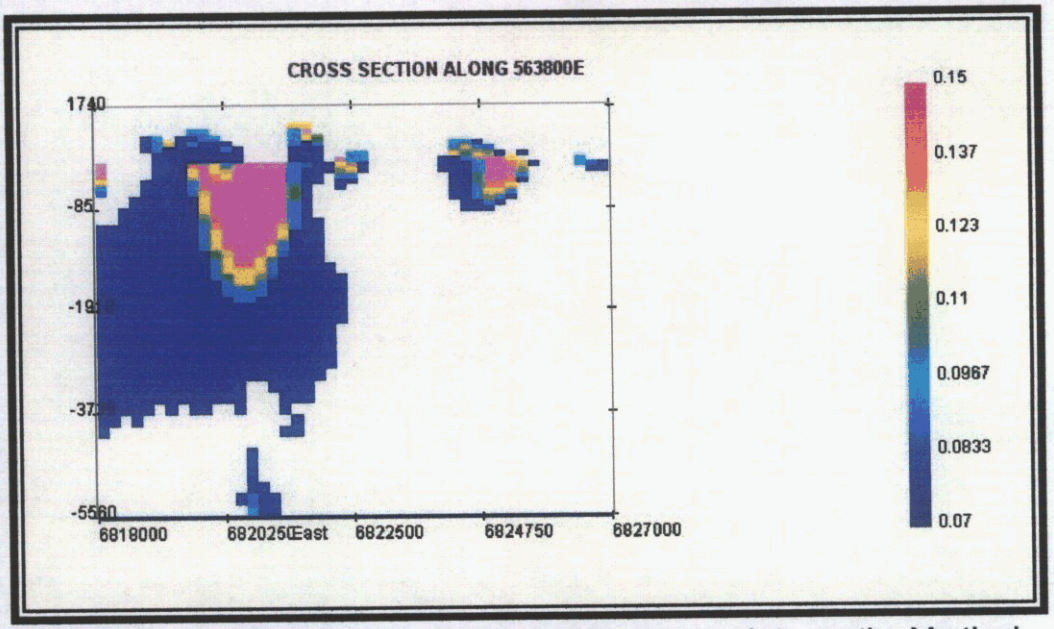

Figure 11. Cross section along 563,800E from south to north. Vertical scale in metres.

Figure 12 is a west (left) to east (right) cross-section along 6,820,400N showing the overall structure of the southern magnetic source.

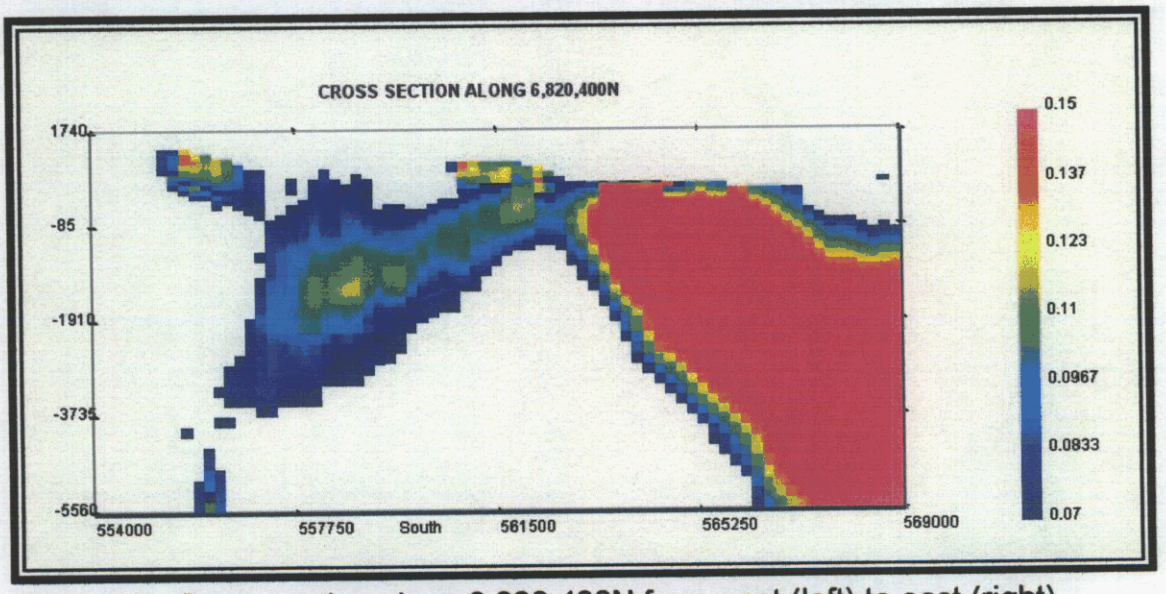

Figure 12. Cross section along 6,820,400N from west (left) to east (right). Vertical scale in metres.

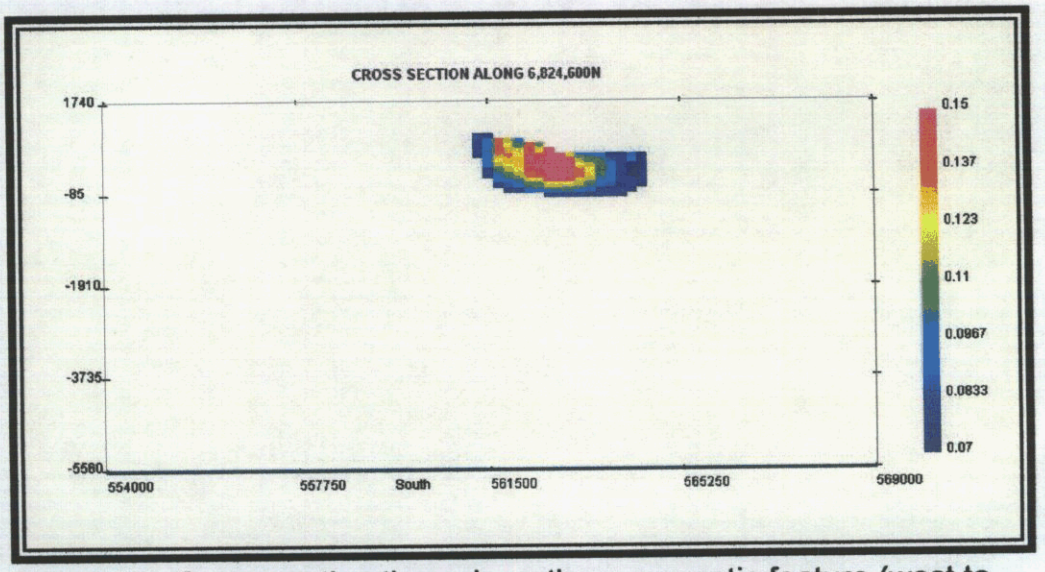

Figure 13. Cross-section through northern magnetic feature (west to east). Vertical scale is metres above mean sea level.

Figure 13 is a cross sectional view along 6,824,600N from west (left) to east (right) through the northern magnetic source. It clearly indicates the modelled limited depth extent of this feature.

The large southern magnetic source is apparently folded about a north-south axis in the middle of the study area and the greater concentration of highly susceptible material is in the eastern portion of the model (Figure 12). This body is also flexure folded about an east-west axis and is concave downward (Figure 9).

The smaller northern magnetic source appears to be depth limited block of highly susceptible material. It may represent a fault bounded slice of magnetically susceptible ultramafic rocks.

The other small features generated in the model are likely not significant. Some are edge effect artifacts generated to explain cut-off anomalies in the data set near the edges of the data set. Others within the model are too small to represent magnetic sources which might be of significant economic interest.

9.0 CONCLUSIONS

The results of the automated inversion of the aeromagnetic data from the Wolv and Don Properties suggest the following conclusions:

a. A large magnetic source in the southern portion of the property is coincident with the Don Property. The recovered model susceptibilities in this area suggest that the source is likely ultramafic rocks with the more susceptible areas - possibly representing peridotite - pyroxenite units - located in the eastern portion of the block.

b. The southern block appears to be folded across a north-south and an east west axis. The culmination occurs in the centre of the study area.

c. A small, highly susceptible magnetic source lies north of the main source. This source has a limited depth extent and is interpreted to be a fault bounded slice of ultramafic rocks.

10.0 RECOMMENDATIONS

The following recommendations are made based on the conclusions of this work:

a. The areas indicated to be underlain by the shallow margins of the two magnetic source blocks should be investigated with large loop transient EM surveys to locate conductors potentially located with basal or offset style massive sulphide mineralization.

Respectfully submitted,
AURORA GEOSCIENCES LTD.

REGISTERED PROFESSIONAL GEOPHYSICIST
LICENSEE
Yukon
N.W.T.

Michael A. Power, M.Sc. P.Geoph.
Geophysicist

REFERENCES CITED

Bhattacharyya, B.K,
1964: Magnetic Anomalies due to prism-shaped bodies with arbitrary polarization. Geophysics, Vol 23, No. 4 (August 1964)

Duncan, R.A. and Tucker, T.L.
2002: 2001 Assessment Report on the Don 1-6, 11-19, 29-34. Unpublished assessment report filed with the Whitehorse Mining Recorder.

Geological Survey of Canada
2004: Digitized aeromagnetic profiles - 115 G. Digitized analog profile data purchased from the GSC registered to NAD83.

Gordey, S.P. and Makepiece, A.J.
1999: Yukon Digital Geology (interactive compact disc). Exploration and Geological Services Division, Yukon: Open File 1999-1D.

Telford, W.M., L.P. Geldart and R.E. Sheriff
1990: Applied Geophysics (2nd Edition) New York: Cambridge University Press.

APPENDIX A. CERTIFICATE

I, Michael Allan Power, with residence and business address in Whitehorse, Yukon Territory do hereby certify that:

1. I hold a B.Sc. (Honours) in Geology granted in 1986 and M.Sc. in Geophysics granted in 1988, both from the University of Alberta.

2. I have been actively involved in mineral exploration in the northern Cordillera and in the Northwest Territories since 1988. I am a professional geoscientist registered with the Association of Professional Engineers and Geoscientists of British Columbia (Registration number 21131) and a professional geophysicist registered with the Northwest Territories Association of Professional Engineers, Geologists and Geophysicists (L942).

3. I conducted the automated inversions described in this report, interpreted the results and prepared this report.

4. I have no interest, direct or indirect, nor do I hope to receive any interest, direct or indirect, in Midnight Mines Ltd. or any of its properties.

Dated this 4th day of October 2004 in Whitehorse, Yukon Territory.

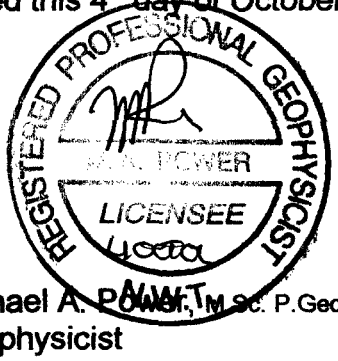

Michael A. Power, M.Sc. P.Geoph.
Geophysicist

APPENDIX B. STATEMENT OF EXPENDITURES

Digital topography & aeromagnetic data	$425
Automated inversions: 36 hrs @ $65	$2,340
Drafting & report preparation	$1,200
Total expenses	***$3,965***

I certify that these expenses are correct to the best of my knowledge.

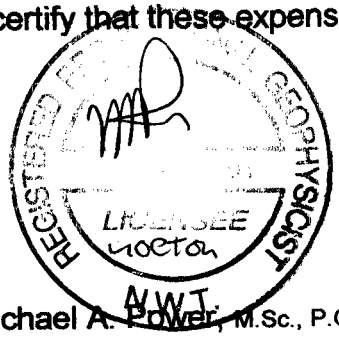

Michael A. Power, M.Sc., P.Geoph.
Geophysicist

554000E 555000E 556000E 557000E -139°55' 558000E 559000E 560000E 561000E -139°50' 562000E 563000E 564000E 565000E 566000E -139°45' 567000E 568000E 569000E

61°34' 6827000N 6826000N 6825000N 6824000N 6823000N 61°32' 6822000N 6821000N 6820000N 6819000N 61°30' 6818000N

WOLV CLAIMS

DON CLAIMS

L1000 E L1010 E L1020 E L1030 E L1040 E L1050 E L1060 E L1070 E L1080 E L1090 E L1100 E L1110 E

0 500 1000 1500 2000

Scale 1:25000

500 0 500 1000 1500
metres
NAD83 / UTM zone 7N

1450.0
1050.0
750.0
600.0
550.0
450.0
350.0
300.0
250.0
200.0
150.0
100.0
50.0
0.0
-50.0
-100.0
-150.0
-200.0
-250.0
-300.0

Residual Magnetic Field
(nT)

RESIDUAL TOTAL MAGNETIC FIELD

Data source: GSC Digitized profiles

Contour intervals: 100, 1000 nT

REGISTERED PROFESSIONAL GEOSCIENTIST
4 OCT 04
N.W.T.

MIDNIGHT MINES LTD.

WOLV & DON PROPERTIES
GSC Aeromagnetic Data
Figure 4. Total Magnetic Field

NTS: 115 G/12
Projection: UTM Zone 7
Date: 01 September 04

Datum: NAD 83
Mining District: Whitehorse
Job: MML-04-001-YT

AURORA GEOSCIENCES LTD.